UDC 622.35:679.8.053

**M. V. SEKRETOV**[1], *Associate Professor, Candidate of Engineering Sciences, mv.sekretov@misis.ru*
**M. G. RAKHUTIN**[1], *Professor, Doctor of Engineering Sciences*

[1]*National University of Science and Technology–NUST MISIS, Moscow, Russia*

# SUBSTANTIATION OF DIAMOND BEAD SHAPES FOR WIRE SAWING MACHINES

*The article substantiates the shapes of diamond beads for wire sawing machines and discusses the forces in the diamond beaded wire saws using the method of vertical displacement of a rotated and shifted parabola for the strength analysis of working members of a sawing machine. The proposed coefficient of change in the normal pressure force is defined as a ratio of the normal-wise distance between the initial and shifted parabolas to the maximal pressure value. Using the current values of the proposed coefficient, the cutting force is determined as function of the coordinates of a stone block being sawed. The method is developed for the vertical displacement of a rotated and shifted parabola, which allows finding the change of the cutting force versus the coordinates of a stone block being sawed at different values of the parabola chord. It is found that with respect to the criteria of strength, diamond bead entry in the cut and movement stability of the bead along the cutting line, the highest strength of the diamond beads is achieved with the beads of the barrel, two-wedge and tapered shapes, and with the cylindrical beads with ellipsoid heel.*

***Keywords:*** *diamond bead shape, natural stone block sawing, diamond beaded wire sawing machine, parabolic cutting path, vertical displacement method for parabola, cutting force, rotated and shifted parabola, strength analysis of diamond beads*
***DOI:*** *10.17580/em.2024.02.17*

## Introduction

Diamond beaded wire saw machines enjoy wide application in recent years at stone mining and processing plants, and have almost pushed out the other types of equipment [1–3]. The machines are meant for preliminary milling and cutting of stone blocks into slabs [4, 6]. A benefit of the extensive use of the machines is the decrease in expenses connected with industrial synthetic diamonds and, accordingly, the cost saving in sawing [7–9]. However, these machines suffer from often failures of its operating member — the diamond beaded wire saw, which greatly decreases productivity of the equipment [7, 10, 11].

One of the ways of increasing reliability of such machines is extension of the service life of diamond beads, in particular, selection and validation of their rational shapes and disuse of the least effective shapes. To this effect, it is required to determine loads [12–14] and stresses [15, 16] generated in the machine system using a more accurate method of force and strength calculation. For finding loads in diamond wire sawing, it is expedient to use the computer graphic model of a parabolic cutting trajectory [17, 18].

Based on the aforesaid, it relevant to substantiate the diamond bead shapes using the proposed method of diamond wire saw strength calculation.

## Methods

The loads in diamond wire sawing were determined using the computer graphic method. The calculations assumed a parabolic trajectory of cutting.

Properties of parabola are widely used in various engineering calculations [19–21]. Generally, parabola is described by the equation:

$$y(x) = -\frac{px^2}{2}, \quad (1)$$

where $p$ is the focal chord of the parabola.

The rotation of the parabola uses the formulas from [19]:

$$\begin{aligned} x' &= x\cos\beta - y\sin\beta, \\ y' &= x\sin\beta + y\cos\beta, \end{aligned} \quad (2)$$

where $x', y'$ are the coordinates of a point shifted in rotation by an angle b relative to the coordinate origin.

The change in the cutting force subject to the horizontal coordinates $x$ is determined graphically, by means of vertical displacement of the parabolic curve of diamond wire sawing at a distance from the parabola (offset curve) to revise the values of forces generated in sawing.

The axis $y$ is formed by an intersection of the plane of cutting and the perpendicular vertical plane of symmetry of a stone block. The axis $x$ passes the peak of the cutting parabola. The current value of the coordinate origin shifts along the axis $y$ with repositioning of the peak of the parabola.

The cutting force $F_{cut}$ is presented as the friction force $F_{fr}$ [14, 22]:

$$F_{cut} = F_{fr} = kN, \text{ N}, \quad (3)$$

where $k$ is the friction factor, $N$ is the normal pressure force, N.

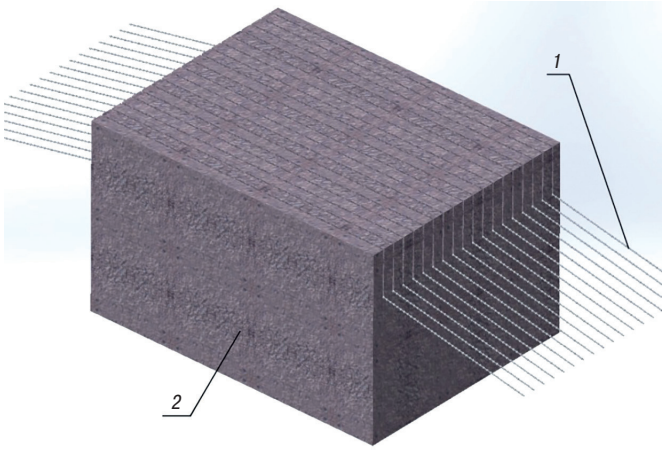


**Fig. 1. Diamond multi-wire saw–stone block model:**
*1* – diamond multi-wire saws; *2* – stone block being cut

The strength analysis of diamond beads [12], based on the force analysis of the diamond wire saw — stone block system, used the model depicted in **Fig 1**.

The main source data for the analysis are the maximal cutting force $F_{cut}$ = 102 N and the normal pressure $N$ = 291.4 N found from formula (3).

Overlapping of forces assumes a lower horseshoe scheme for the worst event in sawing with diamond beads — the bead edge or heel contact with the bottom of saw kerf.

The calculations and plotting used software Mathcad. The strength analysis was performed in the finite element module of software SolidWorks.

## Results and discussion

In diamond wire sawing, the cutting line in the plane of sawing conforms bets of all with the curve of a rotated and shifted parabola, described by the equation derived using formulas (1) and (2):

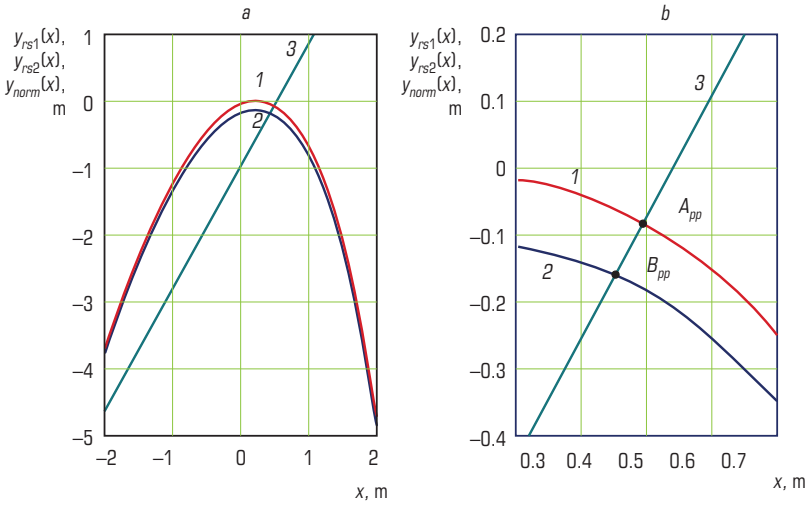


**Fig. 2. Analytical model of vertical shift of rotated and shifted parabolas:**
*a* – analytical model; *b* – intersection of parabola with normal

$$x\sin(\beta)+y\cos(\beta)=-\frac{q\left(x\cos(\beta)-y\sin(\beta)\right)^2}{2}, \quad (4)$$

where β is the angle of rotation of the parabola axis of symmetry relative to the vertical axis at the coordinate origin (0; 0).

Considering the corrective shifts $\Delta x$ and $\Delta y$, the equation of the rotated and shifted parabola curve is given by:

$$y_{rs1}(x)=\left[\frac{1}{2\left(\left(\frac{1}{2}\right)p\sin^2(\beta)\right)}\left[-\left(\cos(\beta)-p(x-\Delta x)\sin(\beta)\cos(\beta)\right)+\right.\right.$$
$$+\left(\left(\cos(\beta)-p(x-\Delta x)\sin(\beta)\cos(\beta)\right)^2-4\left(\left(\frac{1}{2}\right)p\sin^2(\beta)\right)\times\right.$$
$$\left.\left.\times\left((x-\Delta x)\sin(\beta)+\left(\frac{1}{2}\right)p(x-\Delta x)^2\cos^2(\beta)\right)\right)^{\frac{1}{2}}\right]\Bigg]+\Delta y, \quad (5)$$

where $\Delta x = R_{rot}\sin(b)$; $\Delta y = R_{rot}(1-\cos(b))$, $R_{rot}$ is the rotation radius of the parabola.

The analytical model of the vertical shift $\Delta y_2$ of the upper $y_{rs1}(x)$ and lower $y_{rs2}(x)$ rotated and shifted parabolas is shown in **Fig. 2**.

The method of determining the cutting forces $F_{cut}$ consists in the following. The normal pressure force $N$ in formula (3) is proportional to the normal distance from the initial parabola to the second downward-shifted parabola $L_{norm}$, i.e., from the point $A_{pp}$ to $B_{pp}$ in Fig. 2. The change in the force $N$ subject to the coordinate $x$ can be found using the proposed coefficient of the normal pressure force change, $K_N$, as a ratio of $L_{norm}$ to the maximal value $L_{norm\ max}$. In this manner, in conformity with formula (3), the dependence of the cutting force $F_{cut}$ on the coordinate $x$ is determined.

For calculating the cutting forces, two sawing parabolas *1* and *2* are plotted with normal *3* at an arbitrary point (see Fig. 2).

The equation of the parabola 1 $y_{rs1}(x)$ has the form of formula (5), and the equation of the parabola 2 $y_{rs2}(x)$ is given by:

$$Y_{rs2}(x) = y_{rs1}(x) - \Delta y_2, \quad (6)$$

where $\Delta y_2$ is the value of downward shift of parabola 2.

The equation of normal 3 appears as:

$$y_{norm}(x)=\mathrm{tg}\,\gamma\left(x-\Delta x_{norm}\right)+\Delta y_{norm}, \quad (7)$$

where γ is the angle of the normal, rad; $\Delta x_{norm}$ and $\Delta y_{norm}$ are the corrective shifts of the normal along the axes $x$ and $y$, respectively, m.

Let us discuss the example in Fig. 2*b*, where normal 3 and parabola 1 intersect at the point $A_{pp}$ (0.49; –0.08). The intersection point of normal 3 and parabola 2, $B_{pp}$, is determined by solving the system of equations (5), (6) and (7). It is difficult to solve this system analytically. Therefore, the calculations used the function Find meant for solving nonlinear equations in software Mathcad. In the example, $B_{pp}$ (0.448; –0.158).

The distance between the parabola $y_{rs1}(x)$ to the parabola $y_{rs2}(x)$ along normal 3 is calculated from the formula:

$$L_{norm\ pp}=\sqrt{\left(x_{A_{pp}}-x_{B_{pp}}\right)^2+\left(y_{A_{pp}}-y_{B_{pp}}\right)^2}, \quad (8)$$

the example, $L_{norm\ AB\ pp} = 0.090$ m.

The normal pressure force change coefficient is:

$$K_{N\ AB\ pp}=\frac{L_{norm\ AB\ pp}}{\Delta y_2}=\frac{0.090}{0.100}=0.900. \quad (9)$$

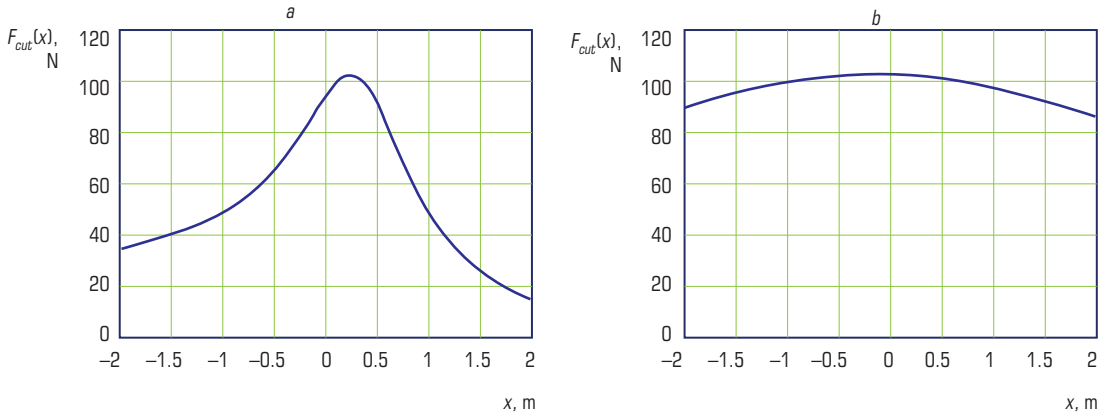


**Fig. 3. Cutting force versus coordinate *x*:**
*a* – $p = 2.0$; *b* – $p = 0.3$

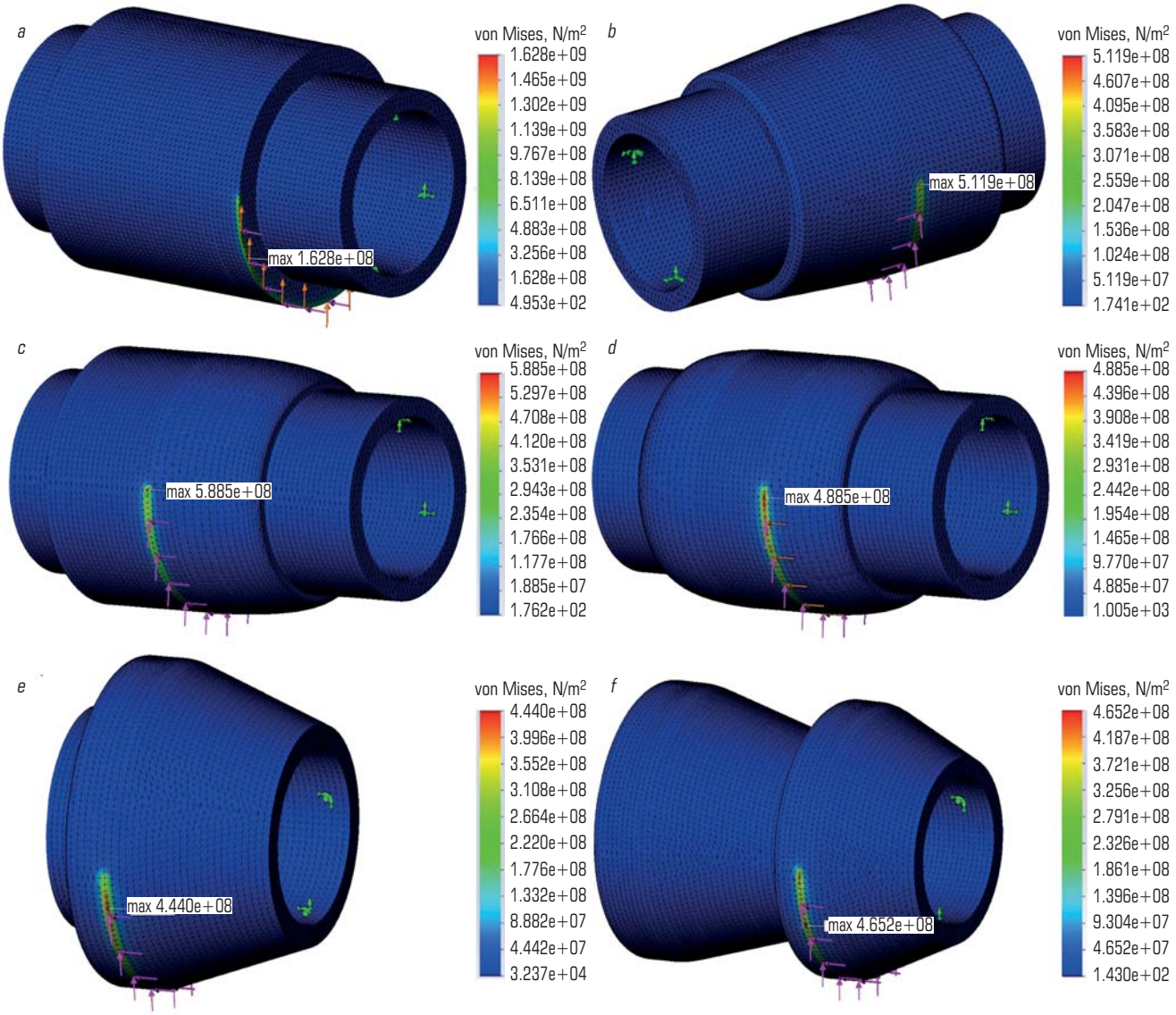


**Fig. 4. Stress distribution diagram for diamond beads:**
*a* – cylinder with sharp edges; *b* – tapered cylinder with rounded edges; *c* – cylinder with ellipsoid heel; *d* – barrel; *e* – wedge; *f* – two wedge bead

Let us calculate the distance $L_{norm\ pp}$ and the coefficient $K_N$ at the other points at a certain preset pit along the axis *x*. The connection of the points using splines in Mathcad [23] produces the spline-interpolation function $K_{N\ pp}(x)$. Since the normal pressure force *N* is proportional to the cutting force $F_{cut}$, the spline-interpolation function $K_{N\ pp}(x)$ is proportional to the cutting force change function $F_{cut}(x)$. The calculated maximal cutting force $F_{cut\ max} = 102$ N. The cutting force dependence on the coordinate *x* is found from the formula:

$$F_{cut}(x) = F_{cut\ max}\, K_{N\ pp}(x). \quad (10)$$

The curves of the cutting forces $F_{cut}(x)$ and coordinates *x* in sawing a stone block at the focal chord values of 0.3 and 2 are plotted in **Fig. 3**.

Such approach to force calculation is sufficiently accurate at high values of the wire saw pre-tension forces $F_{tens} = 1000$–$2000$ N. When the pre-tension forces are low, the maximal cutting forces tend to shift toward the driving drum, which can lead to the egress of the diamond beaded wire saw from the cut during operation.

The strength analysis results obtained in SolidWorks are shown as stress distribution diagrams in **Fig. 4**. In the figure, green color depicts the rigid connections, and the purple and orange arrows show the response of the forces $F_{cut}$ and *N*, respectively.

The maximal stresses were $\sigma_{max\ sh} = 1628$ MPa in a cylindrical diamond bead with sharp edges, $\sigma_{max\ tap} = 512$ MPa in a tapered cylinder diamond bead, $\sigma_{max\ bell} = 589$ MPa in case of an ellipsoid bead heel, $\sigma_{max\ bar} = 489$ MPa in a barrel-like diamond bead, $\sigma_{max\ wed} = 444$ MPa in a wedge diamond bead, and $\sigma_{max\ 2wed} = 465$ MPa in a two-wedge diamond bead.

The obtained values of stresses should be compared with the bonding strength of the diamond layer of a bead. In sawing strong abrasive rocks like granite, the cobalt-based bonding M6-05 with the hardness HRC = 38.8 is used [24].

This index agrees with the tensile stress $\sigma_t \approx 950$–$1000$ MPa, yield stress $\sigma_y \approx 500$–$600$ MPa and the endurance limit stress $\sigma_{-1} \approx 300$–$400$ MPa.

When stresses in diamond beads exceed the yield stress, their sharp and round edges get worn very rapidly first, and the beads break down

quickly already in early operation. The longest service life of diamond beads is attained at stresses lower than the endurance limit stress.

The obtained data analysis brings a conclusion that the cylindrical diamond beads with sharp edges are unadvised for the use as their operation induces high stresses at contact surfaces and they break down fast. The cutting beads of the barrel-like, wedge and two-wedge shapes are the most preferred by the criterion of strength. The tapered cylinders and cylinders with ellipsoid heels are the least preferred.

All test diamond beads are to be qualified with respect to the other criteria, too. By the criterion of the bead entry in the cut, it is advisable to use the barrel-shaped beads, tapered cylinder-shaped beads and the cylinder-shaped beads with ellipsoid heels. The wedge and two-wedge beads are less preferred. By the criterion of stable movement of a diamond bead in a cut, the barrel-shaped beads, tapered cylinder-shaped beads, two-wedge beads and the cylinder-shaped beads with ellipsoid heels are the most expedient. The tapered cylinder-shaped beads fail to ensure stable movement.

The cylinder-shaped diamonds beads with sharp edges fail to meet any of the listed criteria.

## Conclusions

The equation of a rotated and shifted parabola is obtained, and it best defines the sawing trajectory in strong rock blocks in stable speed operation.

The coefficient of change in the normal pressure forces is defined as a ratio of normal-wise distance between the initial and shifted parabolas to the maximal distance.

Based on the current values of the proposed coefficient, it is possible to determine the stone cutting force depending on the cut block coordinates.

The computer graphic method is developed for displacing vertically a rotated and shifted parabola, which allows finding the change in the cutting forces as function of the coordinates of a rock block subjected to sawing at different values of the focal chord of the parabola.

The proposed method of the vertical displacement of the rotated and shifted parabola makes it possible to most accurately determine loads applied to the working members of sawing machines in the course of the strength analysis of the diamond beaded wire saw components.

With respect to the criteria of strength, entry of beads in block cuts and stability of the bead movement along the cutting line, the most efficient use of the cutting members is achieved with the diamond beads of the barrel, two-wedge, tapered shape and with the ellipsoid bead heel. The diamond beads with sharp edges are the least expedient to use in terms of the listed criteria.

*References*


1. Pershin G. D., Karaulov G. A., Karaulov N. G. Diamond rope sawing of marble blocks. Magnitigirsk : MGTU im. G. I. Nosova, 2003. 103 p.
2. Dassanayake A. B. N., Samarakoon A. U., Chaminda S. P. et al. A review on dimension stone extraction methods. *Mining*. 2023. Vol. 3. pp. 516–531.
3. Konstanty J. The mechanics of sawing granite with diamond wire. *The International Journal of Advanced Manufacturing Technology*. 2021. Vol. 116. pp. 2591–2597.
4. Giuseppe Lucisano. Studio e sperimentazione di leghe ad elevata deformazione per applicazioni nel settore della prima lavorazione di materiali lapidei. *Alma Mater Studiorum Universit di Bologna. Dottorato di ricerca in Meccanica e scienze avanzate dell'ingegneria: progetto n. 4 "Meccanica dei materiali e processi tecnologici"*. 2012. 68 p. DOI: 10.6092/unibo/amsdottorato/4839
5. Pershin G. D., Karaulov N. G., Ulyakov M. S. Selection of high-strength dimension stone cutting method, considering natural jointing. *Journal of Mining Science*. 2015. Vol. 51, No. 1. pp. 129–137.
6. Hao Wu. Wire sawing technology: A state-of-the-art review. *Precision Engineering*. 2016. Vol. 43. pp. 1–9.
7. Pershin G. D., Ulyakov M. S., Pshenichnaya E. G., Gabbasov B. M. Energy based diamond cutting machine performance calculation method used for facing stone extraction. *Vestnik of Nosov Magnitogorsk State Technical University*. 2016. Vol. 14, No. 2. pp. 18–24.
8. Pershin G. D., Ulyakov M. S. Analysis of the effect of wire saw operation mode on stone cutting cost. *Journal of Mining Science*. 2014. Vol. 50, No. 2. pp. 310–318.
9. Pavlov Yu. A., Svetlyakov A. V., Motorny I. N. Decorative stone industry: Global situation and prospects in Russia. *MIAB*. 2022. No. 1. pp. 162–178.
10. Gomes D., Araujo A., Marques R., Patricio J., Lopez V., et al. Damage and failure evaluation of diamond wire for multi-wire sawing of hard stone blocks through modelling and numerical simulation. *MATEC Web Conferences*. 2021. Vol. 349. ID 04001.
11. Denkena B., Bergmann B., Rahner B.-H. A novel tool monitoring approach for diamond wire sawing. *Production Engineering*. 2022. Vol. 16. pp. 561–568.
12. Lan Zhang, Cong Ru, Liquan Wang, Zhengbin Zhu, Chengqiang Zhao. Analysis of impact characteristics of diamond-beaded rope and its influence on cutting efficiency and life. *Journal of Physics Conference Series*. 2019. Vol. 1187, Iss. 3. ID 032067.
13. Huiping Liang, Jiahao Feng, Jianwei Liu, Shuai Zhang, Guanghua Mao. Analysis of adaptive adjustment mechanism for diamond beaded rope of wire saw. *Science of Advanced Materials*. 2022. Vol. 14, No. 11. pp. 1756–1769.
14. Tengyun Liu, Peiqi Ge, Wenbo Bi, Yufei Gao. A new method of determining the slicing parameters for fixed diamond wire saw. *Materials Science in Semiconductor Processing*. 2020. Vol. 120. ID 105252.
15. Rasti A., Adarmanabadi H. R., Sahlabadi M. R. Effects of controllable and uncontrollable parameters on diamond wire cutting performance using statistical analysis: A case study. *Rudarsko-geološko-naftni zbornik*. 2021. Vol. 36, No. 4. pp. 21–32.
16. Mengguang Fu, Peng Zhang, Fei Wang. Modal analysis and experimental investigation into vibration of the diamond-beaded rope based on lumped mass. *Journal of Low Frequency Noise Vibration and Active Control*. 2022. Vol. 41, Iss. 1. pp. 12–26.
17. Liu B. C., Zhang Z. P., Sun Y. H. Sawing trajectory and mechanism of diamond wire saw. *Key Engineering Materials*. 2004. Vol. 259-260. pp. 395–400.
18. Sung Kwon Ahn. Framework for investigating wire saw rock cutting. *International Journal of Machine Tools and Manufacture*. 2020. Vol. 155. ID 103581.
19. Belotserkovskiy D. L. Second-order curves on plane : Instructional guidelines. Moscow : RGU nefti i gaza im. I. M. Gubkina, 2009. 42 p.
20. Korn G., Korn T. Mathematics Reference Book for Researchers and Engineers. Moscow : Nauka, 1973. 832 p.
21. Blinova I. V., Popov I. Yu. Curves Set Parametrically and in Polar Coordinates. Teaching Aid. Saint Petersburg : Universitet ITMO, 2017. 56 p.
22. Lu-Lu Wang, Yong-Chen Pei, Hang Zhang. et al. An improved normal sawing force model with spherical abrasive particles for ultrasonic assisted inner diameter sawing. *Research Square*. 2022. DOI: 10.21203/rs.3.rs-1969167/v1
23. Dyakonov V. P., Abramenko I. V. Mathcad 8 PRO in Mathematics, Physics and in the Internet. Moscow : Nolidzh, 2000. 512 p.
24. Sychev Yu. I., Berlin Yu. Ya. Stone Cutting, Shaping, Polishing and Finishing. Moscow : Stroyizdat, 1985. 312 p.